

## Original Research

## Tozasertib activates anti-tumor immunity through decreasing regulatory T cells in melanoma

Qiaoling Wang<sup>a,1</sup>, Wuyi Liu<sup>b,1</sup>, Huyue Zhou<sup>b</sup>, Wenjing Lai<sup>b</sup>, Changpeng Hu<sup>b</sup>, Yue Dai<sup>b</sup>, Guobing Li<sup>b</sup>, Rong Zhang<sup>b,\*</sup>, Yu Zhao<sup>a,\*</sup>

<sup>a</sup> Department of Pharmacy, University Town Hospital Affiliated of Chongqing Medical University, Chongqing, China

<sup>b</sup> Department of Pharmacy, The Second Affiliated Hospital of Army Medical University, Chongqing, China



## ARTICLE INFO

## Keywords:

Aurora kinase  
Immune checkpoint  
Immune infiltration  
Single-cell analysis  
Tumor microenvironment

## ABSTRACT

Although immune checkpoint therapy has significantly improved the prognosis of patients with melanoma, urgent attention still needs to be paid to the low patient response rates and the challenges of precisely identifying patients before treatment. Therefore, it is crucial to investigate novel immunosuppressive mechanisms and targets in the tumor microenvironment in order to reverse tumor immune escape. In this study, we found that the cell cycle checkpoint Aurora kinase B (AURKB) suppressed the anti-tumor immune response, and its inhibitor, Tozasertib, effectively activated T lymphocyte cytokine release *in vitro* and anti-tumor immunity *in vivo*. Tozasertib significantly inhibited melanoma xenograft tumor growth by decreasing the number of inhibitory CD4<sup>+</sup> T<sub>reg</sub> cells in the tumors, which, in turn, activated CD8<sup>+</sup> T cells. Single-cell analysis revealed that AURKB suppressed anti-tumor immunity by increasing MIF-CD74/CXCR4 signaling between tumor cells and lymphocytes. Our study suggests that AURKB is a newly identified anti-tumor immunity suppressor, whose inhibitors may be developed as novel anti-tumor immunity drugs and may have synergistic anti-melanoma effects with immune checkpoint therapies.

## Introduction

Melanoma, one of the most lethal malignant neoplasms with a poor 5-year survival rate, is an extremely aggressive malignancy that originates from the malignant transformation of melanocytes [1,2]. According to global cancer statistics, there were approximately 325,000 new cases of melanoma and 57,000 new deaths in 2020 [3]. Patients with advanced melanoma who have lost the opportunity for surgical intervention are left with only drug-based treatment options such as immunotherapy and targeted therapies. Among these, three types of anti-tumor immunotherapies have emerged as prominent strategies for melanoma treatment: adoptive cell therapy, immune checkpoint blockade, and vaccination [4–6]. Immune checkpoint inhibitors (ICIs) improve the prognosis of advanced melanoma patients [7]. However, immune checkpoint blockade (ICB) has been constrained by low response rates in patients with melanoma, and the non-specific *in vivo* distribution of ICIs hinders therapeutic efficacy while raising the risk of side effects [8,9]. Recognizing the challenges in developing novel drugs,

our focus has shifted toward exploring the immune-related functions of existing anti-tumor drugs with the aim of identifying drugs that could enhance tumor immunotherapy.

In this study, we first determined the crucial genes involved in immune regulation in melanoma and used a variety of bioinformatic analyses based on sequencing data from melanoma patients. We combined weighted gene co-expression network analysis (WGCNA), differential gene expression analysis, literature CRISPR/gRNA library collection, survival analysis, and tumor immune infiltration score analysis, and found that Aurora kinase B (AURKB) is a crucial gene in modulating anti-tumor immunity in melanoma. AURKB is a serine/threonine kinase required for cell cycle progression that is predominantly expressed in mitotic eukaryotic cells [10]. Its elevated expression is linked to tumorigenesis, cancer development and even metastasis [11]. Tozasertib, a special molecular inhibitor of Aurora kinase, has been shown to effectively disrupt the cell cycle and inhibit tumor growth in a variety of cancer types [12]. In immune regulation, AURKB has been implicated in the control of macrophage polarization and promotion of B cell

\* Corresponding authors.

E-mail addresses: [xqpharmacylab@126.com](mailto:xqpharmacylab@126.com) (R. Zhang), [zhaoyu@hospital.cqmu.edu.cn](mailto:zhaoyu@hospital.cqmu.edu.cn) (Y. Zhao).

<sup>1</sup> These authors contributed equally to this work.

apoptosis [13,14]. However, the role of AURKB in modulating T cell anti-tumor immune responses remains unknown. Tozasertib was used as a potent inhibitor to examine the role of Aurora B kinase [15]. T lymphocytes mainly consist of CD4<sup>+</sup> and CD8<sup>+</sup> T cells, both of which play essential roles in anti-tumor immune responses. CD8<sup>+</sup> T cells specifically recognize endogenous antigen major histocompatibility complex (MHC) class I complexes, whereas CD4<sup>+</sup> T cells recognize exogenous antigenic peptides presented by MHC class II molecules [16]. Upon recognition, they differentiate into cytotoxic T lymphocytes (CTLs) that target and eliminate tumor cells. However, a substantial subset of CD4<sup>+</sup> T cells, known as regulatory T (T<sub>reg</sub>) cells, play a pivotal role in immunosuppression [17]. They contribute to the formation of an immunosuppressive tumor microenvironment (TME) aimed at mitigating the inflammatory responses resulting from T cell hyperactivity, while also enabling tumor cell immune evasion [18]. Therefore, increasing CD8<sup>+</sup> T-cell cytotoxicity, decreasing the inhibitory function of T<sub>reg</sub> cells, or combining both strategies can effectively enhance the anti-tumor response.

Collectively, the existing evidence proves that Tozasertib is capable of suppressing melanoma; however, whether Tozasertib is an effective drug for T cell-mediated anti-tumor immune response remains unclear. Our research aimed to uncover the relationship between Tozasertib/AURKB and tumor-infiltrating T cells and shed light on their importance in anti-tumor immunity.

## Methods

### Bioinformatics analysis

#### Data download

The Skin Cutaneous Melanoma (SKCM) RNA-seq gene expression datasets were obtained from Cancer Genome Atlas (TCGA) database. The clinical traits of patients with SKCM were downloaded from UCSC Xena (<https://xena.ucsc.edu>). The overexpressed genes ( $|\log_2\text{Fold-Change}| \geq 1$  and  $q\text{-value} < 0.01$ ) of SKCM were analyzed in Gene Expression Profiling Interactive Analysis 2 (GEPIA 2, <http://gepia2.cancer-pku.cn/#index>). We chose some important phenotypes that we considered relevant to the melanoma patients, such as pathologic stages, tumor grades, and days to death.

#### WGCNA and Venn analysis

To perform WGCNA, the clinical traits of the patients were filtered for the remaining indicators, such as pathologic stages, tumor grades, and days to death. The expression matrix was then integrated and analyzed using the WGCNA package in the R software. Hub genes negatively correlated with patient prognosis were identified for subsequent analyses. Additionally, we collected potential immunosuppressive genes from the CRISPR/gRNA library screening experiments of 10 relevant articles (Supplementary Table 1). The Venn diagram for key gene screening was generated using Omicstudio online software (<https://www.omicstudio.cn/tool>).

#### Functional enrichment analysis

Gene set cancer analysis (<http://bioinfo.life.hust.edu.cn/GSCA>) was used to determine the relationship between gene expression levels and immune infiltration of SKCM. DAVID Bioinformatics Resources (<https://david.ncifcrf.gov/home.jsp>) were used for Gene Ontology (GO) function and Kyoto Encyclopedia of Genes and Genome (KEGG) pathway analysis. Gene set enrichment analysis (GSEA) was performed using the hallmark genes from the Molecular Signatures Database (<https://www.gsea-msigdb.org>), and  $|\text{NES}| > 1$  and  $P < 0.05$  were considered statistically significant. In addition, Protein-Protein Interaction Networks (PPI) were analyzed using the STRING online website (<https://string-db.org/>) and Cytoscape software.

### Other bioinformatics analysis

The Tumor Immune Estimation Resource (TIMER, <https://cistrome.shinyapps.io/timer/>) was used to estimate the association between gene expression and T lymphocyte tumor infiltration. The overall survival of patients with SKCM and the correlation between gene expression was analyzed using GEPIA. AURKB expression in immune cells was analyzed using the Human Protein Atlas (HPA, <https://www.proteinatlas.org/>). The correlation between gene expression and response to anti-PD1 therapy was analyzed using the GSE168204 dataset in the Gene Expression Omnibus (GEO) database (<https://www.ncbi.nlm.nih.gov/geo/>).

### Single-cell sequencing analysis

Initially, a cohort of single-cell sequencing data from melanoma patients was obtained from the GEO database (GSE174401). Subsequently, the count matrix was analyzed using the Seurat R package with the default parameters. Low-quality cells were filtered using the following criteria: (i) number of detected genes below 500 or over 2,500, (ii) percentage of mitochondrial genes below 5 %, and (iii) number of total UMIs between 1,000 and 40,000. Standard parameters were used for count normalization, principal component analysis (PCA), t-distributed stochastic neighbor embedding (tSNE) analysis, and cell clustering. Cluster-specific genes were identified based on RNA expression using the FindAllMarkers function in Seurat. To annotate different clusters, the cell type-specific gene signatures were used as follows: melanoma cells (PMEL, MLANA, MITF and S100A1); granulocytes: (CEACAM1, ALDH1A3, TSPAN8 and MTIM); fibroblasts: (TAGLN, COL1A1, COL3A1, DCN and COL6A3); dendritic cells (DCs): (CD1C, ITGAX, HLA-DQA1, FCER1A, CLEC10A and CD1E); macrophage cells: (ITGAM, CD14, MRC1 and CD163); B cells: (CD79A, CD19 and CD79B); CD4<sup>+</sup> and CD8<sup>+</sup> T cells: (PTPRC, CD3G, CD3D, CD4 and CD8A). In addition, we divided all single cells into two groups based on AURKB expression and analyzed the effects of different AURKB expression levels on immune cell populations and cell-cell communication. Single-cell communication was analyzed using the standard CellChat R package (<https://github.com/sqjin/CellChat>).

### Cell lines and cell culture

The cell lines were obtained from the American Type Culture Collection (ATCC, Manassas, VA, USA). B16F10 cells were cultured in Dulbecco's modified Eagle's medium (DMEM, Gibco) supplemented with 10 % Fetal Bovine Serum (FBS, LONSER, S711-001S). Jurkat T cells were cultured in RPMI Medium 1640 basic (Gibco, C11875500CP) supplemented with L-glutamine and 10 % FBS. Cell cultures were maintained in an incubator at 37°C with a 5 % CO<sub>2</sub> atmosphere. All cell experiments were conducted during the logarithmic growth phase. For cell passaging, the cells were washed with 1 × PBS and digested with 0.25 % trypsin-ethylenediaminetetraacetic acid (Gibco, 25200072).

### RNA extraction and RT-qPCR

Tozasertib (Selleckchem, S1048) was dissolved in DMSO (Beyotime, ST038) at a concentration of 1 mM as a stock solution. B16F10 cells were treated with Tozasertib at the dosage of 10 μM, then total RNA of the cells was extracted according to the protocol of RNAiso Plus (Takara, 9109) and the concentration was measured by NanoDrop (Thermo, ND-2000c). The qPCR primers were synthesized by Sangon Biotech Company and are listed in Supplementary Table 2. RT-qPCR was performed using a Quantstudio1™ Real-Time PCR instrument (Life Technologies, USA).

### RNA-seq analysis

B16F10 cells were treated with 10 μM Tozasertib or equal volume DMSO for 24 h. Total cell RNA were extracted by RNAiso Plus, and sent

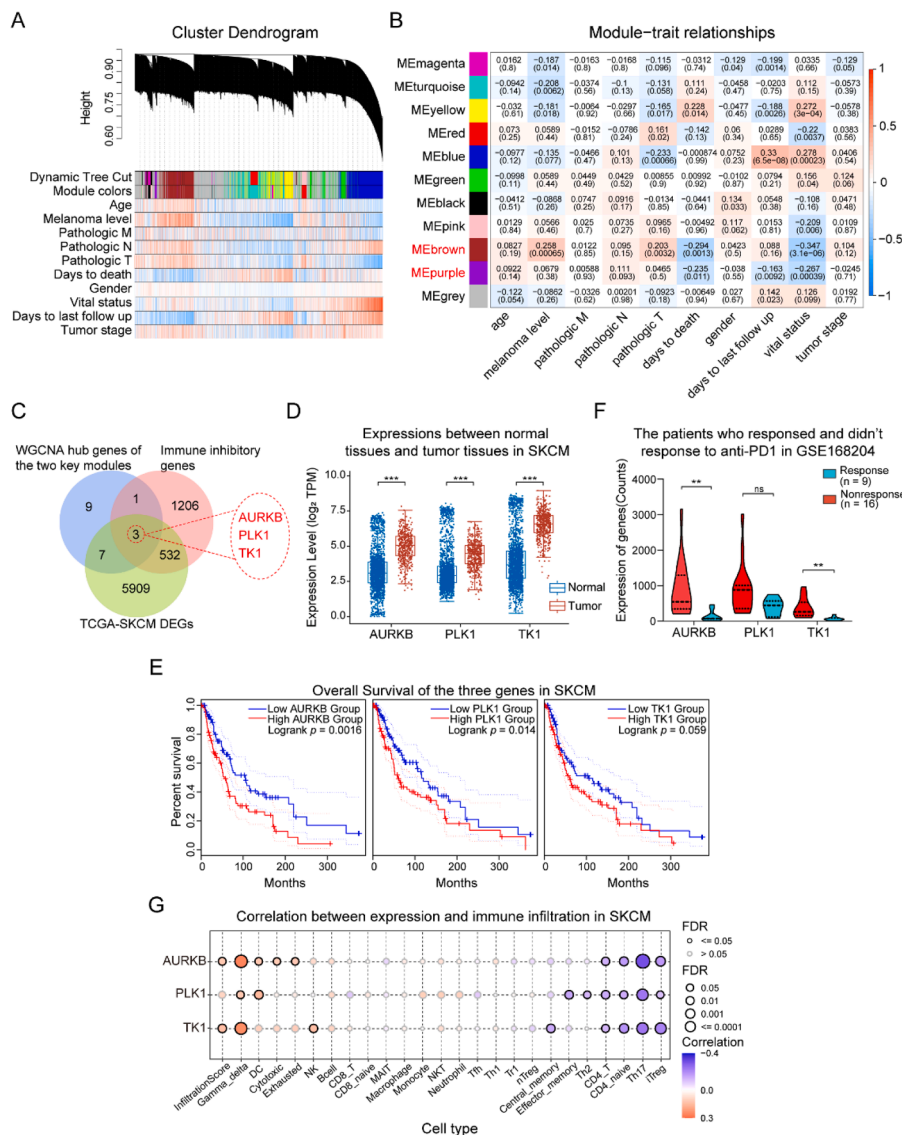


**Fig. 1.** AURKB is a crucial gene in modulating anti-tumor immunity in melanoma. (A, B) Hierarchical cluster dendrograms and heatmaps illustrating the correlation between different modules and clinical traits of Skin Cutaneous Melanoma (SKCM) analyzed by weighted gene co-expression network analysis (WGCNA). (C) Venn diagram was constructed to identify key overlapping genes among WGCNA hub genes, upregulated differentially expressed genes (DEGs) in SKCM, and immunosuppressive genes identified through CRISPR/gRNA library screening. (D) Expression levels of three candidate genes in normal and tumor tissues of melanoma patients as determined by Assistant Clinical Bioinformatics. (E) Overall survival plots of the three candidate genes obtained from GEPIA, with group cutoffs set at the quartile of their expression levels. (F) The relationship between AURKB expression and the effectiveness of anti-PD1 therapy in SKCM patients, using data from the GSE168204 dataset. (G) Gene Set Cancer Analysis (GSEA) depicting the correlation between gene expression and immune infiltration in SKCM.

to the Beijing Genomics Institute (BGI) for RNA-sequencing. Differentially expressed genes (DEGs) were screened (the cut-off value was set as  $p < 0.05$  and  $|\log_2FC| \geq 1$ ).

**Mouse tumor models**

All animal experiments were approved by the Laboratory Animal Welfare and Ethics Committee of Army Medical University. Six-week-old female C57BL/6 mice were used to establish subcutaneous xenograft tumor models under specific pathogen-free (SPF) conditions. Briefly, the mice were subcutaneously inoculated with  $5 \times 10^4$  B16F10 cells in the right flanks. After the tumor became visible, the mice were randomly divided into two groups and intraperitoneally injected with Tozasertib (50 mg/kg) or an equal volume of vehicle daily. Tumor dimensions were measured using a Vernier caliper, and body weight was recorded every other day. The tumor volume was calculated using the following formula:  $\text{length} \times \text{width} \times \text{width} / 2$ . An ethical endpoint for

ethanasia was set at a tumor volume greater than  $2000 \text{ mm}^3$ .

**Flow cytometry analysis**

**Isolating tumor-infiltrating immune cells**

Tumors were harvested from both control and treatment groups. PBS was added to homogenize the tumor tissue into a single-cell suspension by passing a  $70 \mu\text{m}$  strainer. Density-gradient centrifugation was performed using a Percoll centrifuge (Cytiva, 17089109) at  $600 \times g$  for 20 min at room temperature. Immune cells were carefully collected from the middle of the cloudy layer. After washing with PBS, the red blood cells were lysed using Red Blood Cell Lysis Buffer (Beyotime Company, C3702). Afterward, cells were incubated with eBioscience™ Brefeldin A (1000 × Solution, invitrogen, 00-4506-51) and eBioscience™ Monensin (1000 × Solution, invitrogen, 00-4505-51) for 4 h at  $37^\circ\text{C}$  and 5 %  $\text{CO}_2$  to facilitate further intracellular proteins staining.

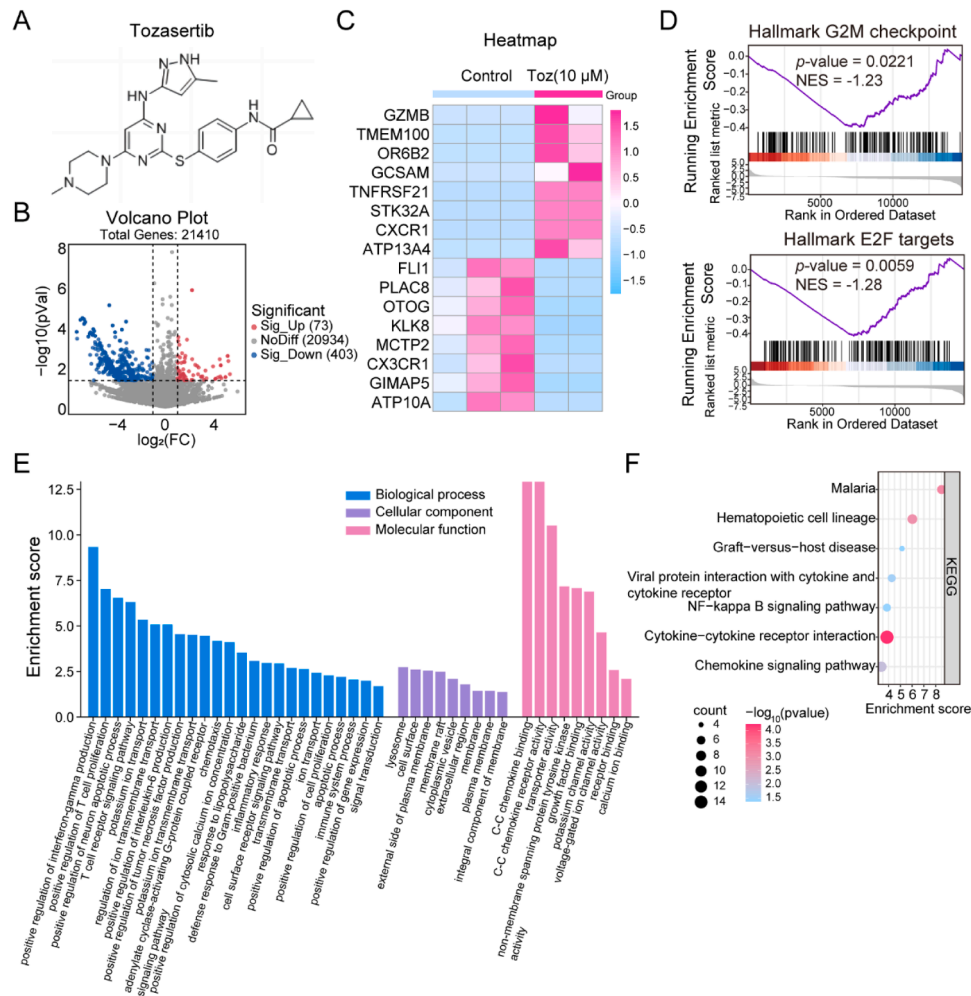


**Fig. 2.** RNA-seq analyzing results of B16F10 cells treated with 10  $\mu$ M Tozasertib. (A) The chemical structure of Tozasertib. (B) Volcano plot illustrating differentially expressed genes (DEGs). (C) Clustered heatmap of DEGs. (D) Key pathways enriched via Gene set enrichment analysis (GSEA). NES, normalized enrichment score. (E) Analysis of Gene Ontology (GO) terms for DEGs. (F) Analysis of Kyoto Encyclopedia of Genes and Genomes (KEGG) pathways for DEGs.

### Staining immune cells and flow cytometry analysis

Immune cell staining and live/dead status were assessed using the antibodies listed in Supplementary Table 3. For intracellular proteins staining, cells were incubated for 20 min in Fixation and Permeabilization Solution (BD Biosciences, 554722), and then stained with anti-IFN- $\gamma$ , anti-TNF- $\alpha$  in 1  $\times$  BD Perm/Wash<sup>TM</sup> Buffer for 20 min at 4°C. FOXP3 was stained with an antibody using the FOXP3/Transcription Factor Fixation/Permeabilization Solution (eBioscience, 00-5521-00). After washing with PBS, samples were analyzed using a flow cytometer (BD LSRFortessa<sup>TM</sup>) and the data were analyzed using FlowJo V10.3 software. The gating strategy for T cells included the initial selection of single cells, followed by the exclusion of dead cells using a live/dead viability dye. Subsequently, T cells were identified based on CD3 positivity, and CD4 and CD8 positive subsets were evaluated by PD1, TIGIT, LAG3, TIM3, CD107a, TNF- $\alpha$  and IFN- $\gamma$  expression.

### H&E staining and immunofluorescence

Tumor, liver, and kidney tissues harvested from tumor-bearing mice were fixed, embedded, sectioned, and stained with hematoxylin and eosin (H&E) or immunofluorescence (IF) staining. For IF staining, T<sub>reg</sub> cells were stained for CD4 (Santa Cruz Biotechnology, sc-19641) and FOXP3 (Cell Signaling Technology, 12653). HMB45 (Santa Cruz, sc-59305) was used to mark melanoma cells. MIF (ImmunoWay Biotechnology Company, YT2761) and CD74 (ImmunoWay Biotechnology

Company, YT5464) were detected. Samples were visualized and images were captured using a fluorescence microscope (Leica, DMi8).

### Statistics analysis

GraphPad Prism 8.0 statistical analysis software was used for statistical analysis in this study. Data are presented as the mean  $\pm$  standard deviation, and statistical significance was defined as  $p < 0.05$  in the unpaired t test.

### Results

*AURKB* is a crucial gene in modulating anti-tumor immunity in melanoma according to bioinformatics analysis

To identify the key genes that modulate immunity in melanoma, a series of bioinformatics analyses were conducted. WGCNA is a systems biology method used to identify potential biomarker genes by identifying modules of gene signatures that share common expression patterns and analyzing their correlation with sample traits [19]. Initially, we performed WGCNA using TCGA SKCM gene expression matrix and patient clinical traits. Several color modules that aggregated highly correlated genes were generated. We then analyzed the correlation between these modules and clinical prognostic indicators to identify hub genes that were negatively associated with patient prognosis. All hub

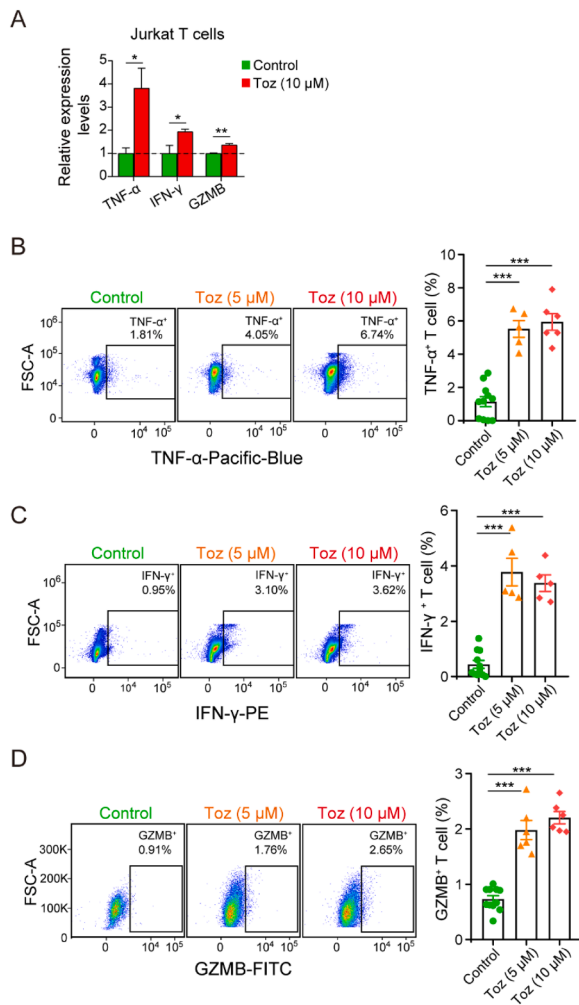


**Fig. 3.** Tozasertib activates T lymphocytes to release cytokines *in vitro*. (A) Jurkat T cells were treated with 10 μM Tozasertib for 24 h. RT-qPCR was used to explore the mRNA transcriptional level of TNF-α, IFN-γ and GZMB. (B–D) Jurkat T cells were treated with 5 μM or 10 μM Tozasertib for 24 h. Flow cytometry was employed to detect the expression of TNF-α, IFN-γ and GZMB.

genes are listed in Supplementary Table 4. Our results revealed that the brown and purple modules were key modules associated with poor prognosis, and we identified 20 hub genes within these modules through weighted analysis (Fig. 1A, B). Furthermore, 6,451 DEGs in SKCM were analyzed and obtained from the GEPIA 2 database. Additionally, we collected 1,742 potential immunosuppressive genes from the relevant literature on CRISPR/gRNA library screening in cancer cells or xenograft mouse models (Supplementary Table 1). A Venn diagram was used to combine these gene sets and ultimately identify three candidate genes (AURKB, PLK1, and TK1) for further analysis (Fig. 1C). Through expression analysis, we observed that all three genes exhibited higher expression levels in melanoma tumor tissues than in normal tissues (Fig. 1D). Based on overall survival analysis, AURKB exhibited a more significant negative association with patient survival than the other two genes (Fig. 1E). Importantly, patients with SKCM with high AURKB expression appeared to be less responsive to anti-PD1 therapy, which was most pronounced among these three genes [20] (Fig. 1F). In addition, GSCA analysis revealed that AURKB expression correlated with immune cell tumor infiltration [21] (Fig. 1G). AURKB is a well-known cell cycle regulator critical for tumor cell division and proliferation. However, its role in regulating tumor immunity remains unclear.

In addition to inhibiting the cell cycle, the anti-cancer activity of Tozasertib may also be achieved by affecting immune response pathway

Tozasertib (MK-0457 or VX-680), a specific small-molecule inhibitor of AURKB, was employed in our study (Fig. 2A). First, we performed RNA-seq analyses of Tozasertib-treated B16F10 cells at the transcriptome level. We identified 73 upregulated and 403 downregulated genes through (DEG) analysis and showed the top eight upregulated and downregulated DEGs in a heatmap (Fig. 2B, C). GSEA revealed that Tozasertib treatment significantly enriched cell cycle associated pathways, including G2M checkpoint and E2F targets [22] (Fig. 2D). Furthermore, GO terms and KEGG pathway analyses revealed that DEGs were significantly enriched in the positive regulation of cell proliferation and various immune-related signaling pathways (Fig. 2E, F). Taken together, our transcriptome sequencing results suggest that Tozasertib treatment not only inhibits the cell cycle but also influences the anti-tumor immune response.

#### Tozasertib activates T lymphocytes to release cytokines *in vitro*

Because we found a potential relationship between Tozasertib and T cells, we tried to determine how T cells would be influenced by Tozasertib. Jurkat T cells were first used to detect changes in cytokine release following Tozasertib treatment. Total RNA was extracted from Tozasertib-treated Jurkat T cells and control cells, and the expression of cytokines, including TNF-α, IFN-γ, and GZMB, was quantified using RT-qPCR. The results revealed that Tozasertib significantly upregulated the transcriptional expression of all three cytokines (TNF-α, IFN-γ, and GZMB) (Fig. 3A). Furthermore, flow cytometry analysis of Tozasertib-treated Jurkat T cells confirmed a substantial increase in the expression of TNF-α, IFN-γ, and GZMB. These findings are consistent with the results of RT-qPCR (Fig. 3B–D). Collectively, these results suggest that Tozasertib activates T lymphocytes and induces cytokine release *in vitro*.

#### AURKB may promote tumor progression by increasing $T_{reg}$ cells in tumor microenvironment

To elucidate the functional role of AURKB in regulating anti-tumor immunity, we first analyzed the correlation between AURKB and immune infiltration levels of  $CD4^+$  and  $CD8^+$  T cells in SKCM using the TIMER database. The results indicated a significant negative correlation between the high AURKB expression and  $CD4^+$  T-cell tumor infiltration in SKCM (correlation:  $-0.289$ ,  $p < 0.05$ ) (Fig. 4A). Additionally, the PPI networks derived from our RNA-seq analysis of Tozasertib-treated B16F10 cells revealed that Tozasertib treatment predominantly affected  $CD4^+$  T lymphocyte-mediated anti-tumor immune responses (Fig. 4B). Furthermore, we examined AURKB across different immune cell types in the HPA dataset, which includes 1,206 cell lines, 40 human tissues, 18 blood cell types, and total peripheral blood mononuclear cells. Our results showed that  $T_{reg}$  cells had significantly higher levels of AURKB expression than other types of immune cells (Fig. 4C). Moreover, we investigated the correlation between AURKB and  $T_{reg}$  cell markers including CD4, FOXP3, IL2RA, CTLA4, IL10, and ITGAE [23–25]. The results demonstrated that AURKB expression and  $T_{reg}$  cell markers were positively correlated (Fig. 4D). Single-cell function enrichment analysis using the Protein Atlas database revealed that AURKB was enriched in  $T_{reg}$  cell cycle regulation (Fig. 4E). Taken together, these results suggest that in addition to its role in regulating the tumor cell cycle, AURKB may promote tumor progression by increasing  $T_{reg}$  cells in the tumor microenvironment, and Tozasertib may decrease  $T_{reg}$  cells to improve anti-tumor immune responses.

#### Tozasertib activated anti-tumor immunity *in vivo* through inhibiting $T_{reg}$ cells

To identify the immunological anti-tumor effects of Tozasertib, we

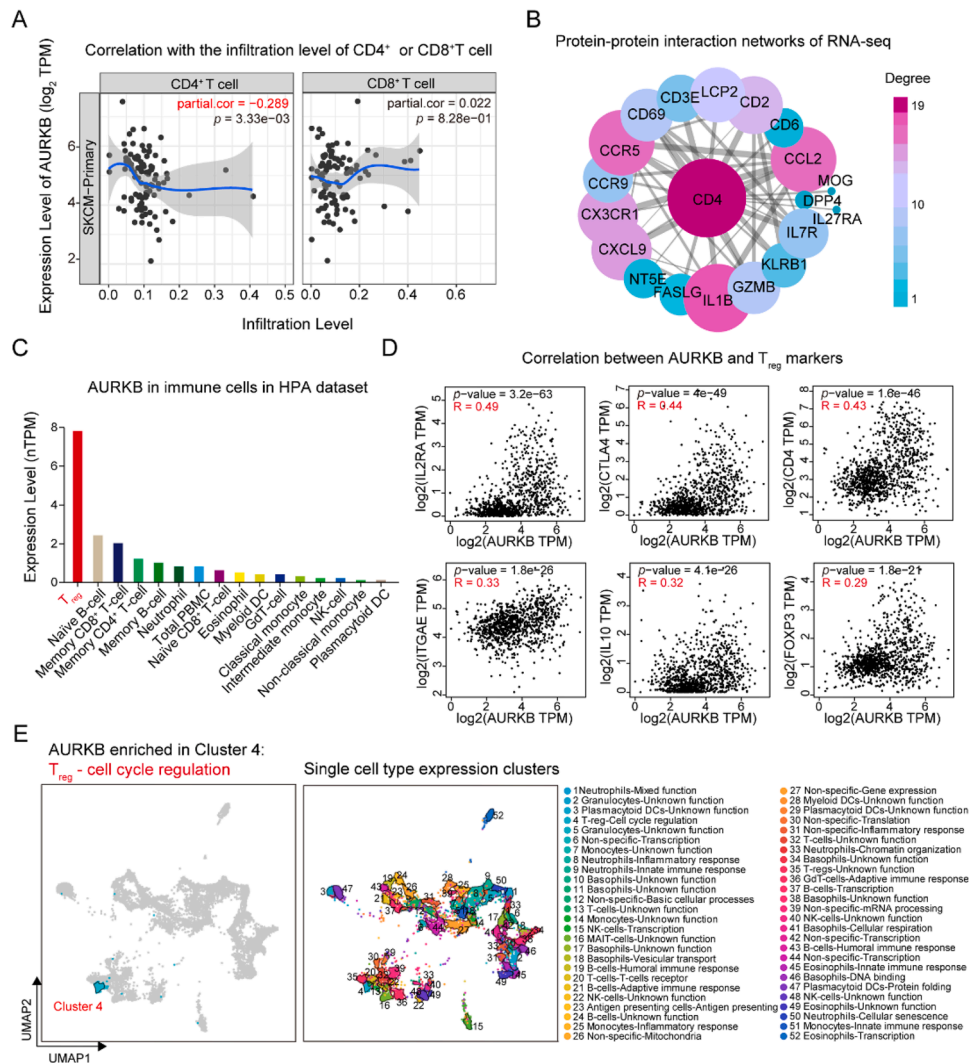


**Fig. 4.** Bioinformatic analysis indicated that AURKB is associated with the T<sub>reg</sub> cells in tumor microenvironment. (A) Correlation between AURKB expression and infiltration levels of CD4<sup>+</sup> or CD8<sup>+</sup> T cells in primary SKCM through using TIMER database. (B) Hub nodes ranked by degree in protein-protein interaction networks analysis of our Tozasertib-treated B16F10 cells RNA-seq. (C) AURKB expression across immune cell types in HPA dataset. (D) Expression correlation analysis between AURKB and T<sub>reg</sub> cells markers. (E) Single-cell function enrichment analysis of AURKB in Protein Atlas database.

established a mouse xenograft model by subcutaneously injecting B16F10 cells. The mice were treated with either a vehicle or Tozasertib at a dose of 50 mg/kg daily. Body weight and tumor volume were measured every alternate day. Treatment of mice with Tozasertib significantly suppressed tumor growth after 7 days of drug exposure (Fig. 5A, B). Notably, there was no significant difference in the body weight between the two groups (Fig. 5C). Subsequently, H&E staining of tumor tissues from mice treated with Tozasertib revealed a reduction in densely packed cells with areas displaying sparse inflammatory/apoptotic/necrotic cells. In contrast, H&E staining of liver and kidney tissues demonstrated that Tozasertib treatment did not induce observable morphological changes (Fig. 5D).

Furthermore, flow cytometry was further employed to detect the markers of tumor-infiltrating lymphocytes (TILs), including T<sub>reg</sub> markers (CD25 and Foxp3), immune inhibitory receptors (PD1, TIGIT, LAG3, TIM3 and CD96) and T cell activation marker TNF- $\alpha$ . Our results revealed that Tozasertib considerably decreased the number of T<sub>reg</sub> cells (CD4<sup>+</sup>, CD25<sup>+</sup>, and Foxp3<sup>+</sup>) and increased the CD8<sup>+</sup> T cells to T<sub>reg</sub> cells (CD8/T<sub>reg</sub>) ratio. Additionally, Tozasertib treatment significantly reduced the proportion of TIGIT<sup>+</sup> and LAG3<sup>+</sup> CD4<sup>+</sup> T cells, plus TIGIT<sup>+</sup> CD8<sup>+</sup> T cells, while enhancing the ratio of TNF- $\alpha$ <sup>+</sup> CD8<sup>+</sup> T cells (Fig. 6A–D).

To further validate the flow cytometry results, which confirmed that Tozasertib treatment decreased the ratio of tumor-infiltrating T<sub>reg</sub> cells, we evaluated B16F10 tumor tissue sections using immunofluorescence staining with anti-CD4 and anti-Foxp3 antibodies. Our results demonstrated that Tozasertib treatment noticeably reduced the population of Foxp3<sup>+</sup> CD4<sup>+</sup> cells, which was consistent with the flow cytometry data (Fig. 7). In summary, our xenograft mouse data strongly suggested that Tozasertib significantly inhibited the proportion of T<sub>reg</sub> cells and enhanced CTLs in tumor tissues.

#### SKCM single-cell analysis inferred that AURKB increases tumor-infiltrated T<sub>reg</sub> cells possibly by enhancing MIF-CD74/CXCR4 signals

To further explore how the expression levels of AURKB influence anti-tumor immunity in patients with melanoma, we downloaded the single-cell dataset GSE174401 for analysis [26]. Initially, we divided the patients into two groups based on the expression levels of AURKB in melanoma cells in each sample. A total of 26,615 cells passed quality control by filtering. Nine cell types were identified using specific markers: granulocytes, melanoma cells, macrophages, mast cells, NK cells, B cells, CD4<sup>+</sup> T cells, CD8<sup>+</sup> T cells, and DCs (Fig. 8A, B, Supplementary Fig. 1A). Subsequently, we annotated the subpopulations of

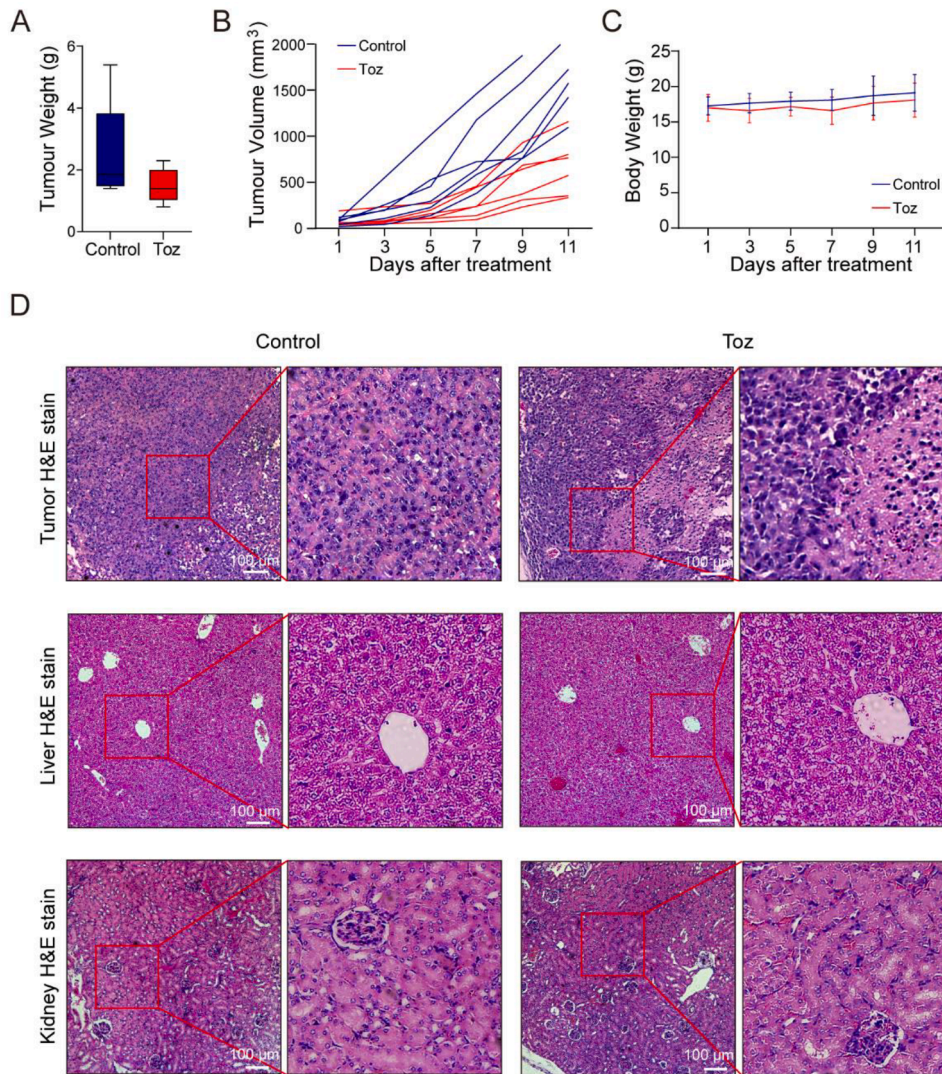


**Fig. 5.** Tozasertib suppressed tumor growth without inducing liver or kidney injury in B16F10 melanoma mice models. B16F10 cells were subcutaneously injected into C57BL/6 mice and divided randomly into two groups ( $n = 6$ ). Mice were treated with Tozasertib or equal volume of vehicle. (A) The weight of tumors. (B) Tumor growth curve of each group during treatment period. (C) Mice body weight curve. (D) Representative H&E-stained tumor, liver, and kidney sections from two groups. Scale bar = 100  $\mu\text{m}$ .

defined lymphocytes (T, B, and NK cells) using typical markers (Fig. 8C, D, Supplementary Fig. 1B). We determined that the proportions of tumor-infiltrating effective  $\text{CD8}^+$  T cells ( $T_{\text{eff}}$ ) and central memory  $\text{CD4}^+$  T cells ( $T_{\text{cm}}$ ) were higher in patients with low AURKB expression than in those with high AURKB expression. Tumor tissues from patients with low AURKB expression contained considerably fewer exhausted  $\text{CD8}^+$  T cells and  $\text{CD4}^+$   $T_{\text{reg}}$  cells (Fig. 8E, F), which confirmed the above results.

Analysis of cell-to-cell communication based on receptor-ligand interactions is a key tool for revealing the underlying molecular mechanism of single-cell analysis [27]. In this study, we used the CellChat R package developed by Jin et al. [28] to infer cell communication pathways. We first analyzed the communications between all identified cell types in melanoma tissues and found that melanoma cells could send signals to eight other cell types, with Macrophage Migration Inhibitory Factor (MIF) being the most important molecule in this process, followed by SPP1 and MDK (Fig. 8G, Supplementary Fig. 2A–D). The circular plot revealed that melanoma cells sent MIF signals to  $\text{CD4}^+$  and  $\text{CD8}^+$  T cells (Fig. 8H). Furthermore, focusing on the MIF signaling pathway, heatmap analysis showed that melanoma cells were the predominant MIF signal sender cells,  $\text{CD4}^+$  T cells were the intermediary mediator cells, and  $\text{CD8}^+$  T cells were the receiver and influencer cells

(Fig. 8I). Subsequently, we identified that the receptor-ligand pairs of the MIF signaling pathway were MIF- $\text{CD74}/\text{CXCR4}$  and MIF- $\text{CD74}/\text{CD44}$  between melanoma cells and  $\text{CD4}^+$  and  $\text{CD8}^+$  T cells (Fig. 8J). Analysis of the DEG in the single-cell type between  $\text{AURKB}^{\text{high}}$  and  $\text{AURKB}^{\text{low}}$  expression levels revealed that MIF was significantly decreased in  $\text{AURKB}^{\text{low}}$  melanoma cells ( $p = 2.2\text{e-}16$ ). Moreover, we found that the expression of both  $\text{CD74}$  and  $\text{CXCR4}$  in  $\text{CD4}^+$  and  $\text{CD8}^+$  T cells was downregulated in the AURKB low-expression group (Fig. 8K). In short, single-cell analysis revealed that AURKB increased the number of tumor-infiltrating  $T_{\text{reg}}$ , possibly by enhancing the MIF- $\text{CD74}/\text{CXCR4}$  signaling pathway between melanoma cells and  $\text{CD4}^+$ / $\text{CD8}^+$  T cells.

To verify our hypothesis, we conducted an immunofluorescence analysis of tumors from control and Tozasertib-treated mice. We found that Tozasertib decreased MIF expression in melanoma cells, which were marked by HMB45 staining (Fig. 8L). Immunofluorescence staining revealed that  $\text{CD74}$  expression on the surface of  $\text{CD4}^+$  T cells was downregulated after Tozasertib treatment (Fig. 8M).

## Discussion

Metastatic melanoma is known for its high mortality rates. Anti-

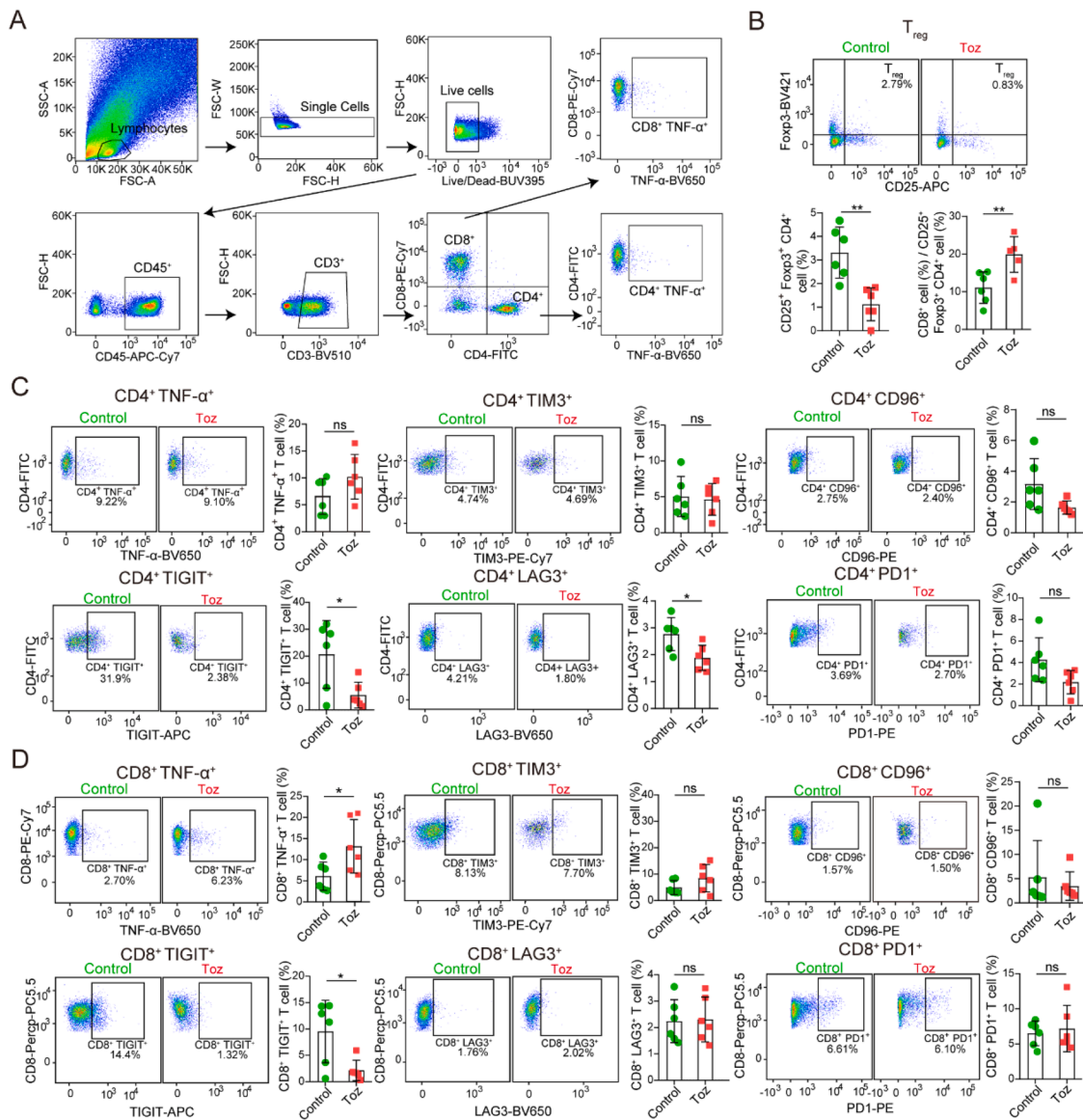


**Fig. 6.** Tozasertib promoted anti-tumor immunity by inhibiting T<sub>reg</sub> cells in B16F10 xenograft mouse model. (A) Gating strategy. (B) The percentage changes of tumor-infiltrated T<sub>reg</sub> cells and the CD8<sup>+</sup> T cell to T<sub>reg</sub> cells ratio. (C) Immune inhibitory receptors (PD1, TIGIT, LAG3, TIM3 and CD96) and T cell activation marker TNF- $\alpha$  expression on CD4<sup>+</sup> T cells. (D) Immune inhibitory receptors (PD1, TIGIT, LAG3, TIM3 and CD96) and TNF- $\alpha$  expression on CD8<sup>+</sup> T cells.

tumor immunotherapy, as represented by ICIs and CAR-T cells, has achieved favorable therapeutic outcomes and has advanced rapidly in recent years [29]. However, owing to its low response rate, immunotherapy has encountered hurdles in melanoma. Tumors that do not respond to checkpoint blockade are frequently infiltrated by suppressor immune cells, especially T<sub>reg</sub> cells and tumor-associated macrophages (TAMs), which compose the TME [30]. Therefore, there is an urgent need for the development of more effective immunotherapy medications to diminish these suppressive cells in the TME and mitigate the growing mortality of melanoma patients.

Through a series of integrated bioinformatics analyses based on the RNA-seq data of melanoma patients, their clinical prognostic data, and potential immunosuppressive molecules from CRISPR/gRNA library screening, we identified the cell cycle checkpoint AURKB as a key molecule that simultaneously suppresses anti-tumor immunity. Aurora kinases, including Aurora A (AURKA), Aurora B (AURKB) and Aurora C (AURKC), are involved in a variety of critical biological processes, including mitosis, spindle assembly and maintenance, centrosome maturation and separation, chromosome segregation, and cytokinesis

[31]. The increased expression of these genes is closely related to tumorigenesis and patient prognosis. Thus, Aurora kinase inhibitors are frequently employed in cancer treatments in mouse models, as well as in anti-tumor clinical trials, including AML, CML, PC, and OV [32–35]. However, whether AURKB and its inhibitor, Tozasertib, are involved in modulating the anti-tumor immune response remains unclear. Punt et al. reported that Aurora kinase could be a mediator of melanoma cell resistance to T cell-mediated cytotoxicity and that inhibition of Aurora kinase synergizes with T-cell-mediated cytotoxicity *in vitro* [36]. Another study revealed that AURKA deletion or pharmacological inhibition slowed tumor growth, which was accompanied by an increase in tumor-infiltrating CD8<sup>+</sup> T cells, and that anti-tumor effects were diminished in the absence of CD8<sup>+</sup> T cells [37,38]. In addition, AURKA inhibition has been shown to abolish the immunosuppressive effects of myeloid-derived suppressor cells (MDSC) and improve the anti-breast cancer efficacy of Anti-PD-L1 [39]. In our study, we found that AURKB expression was consistent with immune cell tumor infiltration and that melanoma patients with high AURKB expression were more unresponsive to anti-PD1 therapy than patients with low AURKB

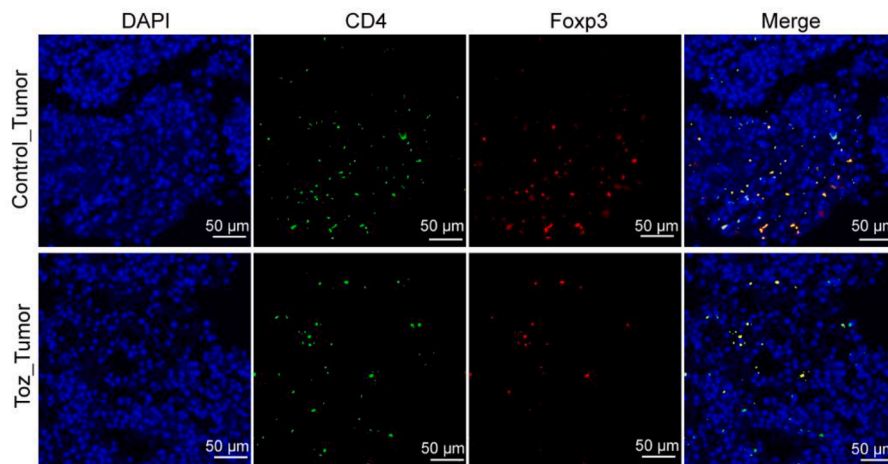


**Fig. 7.** Tozasertib reduced the ratio of  $T_{reg}$  cells demonstrated by immunofluorescence assays. Staining with anti-CD4 and anti-Foxp3 antibodies in B16F10 tumor tissue sections. Scale bar = 50  $\mu$ m.

expression. In addition, our pathway enrichment analysis showed that Tozasertib-treated B16F10 cells were associated with positive regulation of the anti-tumor immune response. More importantly, our data indicated that Tozasertib could activate T lymphocytes to release cytokines *in vitro* and *in vivo*.

$T_{reg}$  cells are a subset of  $CD4^{+}$  T cells characterized by the expression of FOXP3 and CD25 that play immunosuppressive roles in preserving self-tolerance.  $T_{reg}$  cells can inhibit the anti-cancer immunity in tumor-bearing hosts, thereby preventing protective immunosurveillance of tumor cells, and contributing to increased tumor growth and progression through secreting IL10 and TGF- $\beta$  [40]. We revealed for the first time that AURKB promotes tumor progression by increasing the number of  $T_{reg}$  cells in the tumor microenvironment. First, AURKB expression was positively correlated with  $T_{reg}$  cell markers such as CD4, FOXP3, IL2RA, CTLA4, IL10, and ITGAE. Single-cell function enrichment analysis also suggested that AURKB was enriched in  $T_{reg}$  cell cycle regulation. Secondly, both flow cytometry and immunofluorescence staining showed that Tozasertib significantly decreased the number of  $T_{reg}$  cells in B16F10 tumors. Third, single-cell analysis of melanoma patients further verified that tumors with reduced AURKB expression had fewer  $CD4^{+}$   $T_{reg}$  cells. In addition, the cell-to-cell communication in our single-cell analysis revealed that  $CD4^{+}$  T cells function as intermediary mediator cells between melanoma cells and  $CD8^{+}$  T to transmit signals in melanoma tumors. Combined with our *in vivo* xenograft flow cytometry results, we propose that Tozasertib may indirectly raise the ratio of activated  $CD8^{+}$  T cell secreting TNF- $\alpha$ , and reduce the proportion of TIGIT $^{+}$   $CD8^{+}$  T cells, by reversing the immunosuppressive microenvironment through the suppression of  $T_{reg}$  cells.

Macrophage migration inhibitory factor (MIF) is a glycoprotein that contributes to the anti-inflammatory, immunological tolerance, and immunosuppressive TME in malignant cancers. MIF is overexpressed in various solid tumors and promotes neoangiogenesis in tumors [41,42]. Inhibiting MIF expression in tumor cells can effectively reduce tumor progression. In advanced melanoma, MIF contributes to immune evasion and tumor growth by recruiting a large number of immune-suppressed cells to the TME and inducing inhibitory immune cell differentiation [43]. Mechanistically, extracellular MIF interacts with the membrane receptors CD74, CD44, and CXCR4 to form a heterocomplex and subsequently initiates downstream MAPK and/or PI3K pathway effectors. A non-peer-reviewed study implicated CD74 as a driver of metastasis in melanoma [44]. Carlos et al. revealed that blocking MIF-CD74 in macrophages and dendritic cells restored the anti-tumor immune response against melanoma [45]. Our single-cell analysis demonstrated that MIF-CD74/CXCR4 signal communication is the most crucial receptor-ligand pair in the tumor tissues of patients with

melanoma, where melanoma cells act as MIF signal sender cells and  $CD4^{+}/CD8^{+}$  T cells act as signal-receiver cells. Moreover, we found that, compared to the high AURKB expression group, low AURKB expression significantly decreased MIF expression in melanoma cells and significantly decreased both CD74 and CXCR4 expression in  $CD4^{+}$  T and  $CD8^{+}$  T cells. These data suggest that AURKB increases tumor-infiltrating  $T_{reg}$  cells possibly by enhancing MIF-CD74/CXCR4 signaling. Our results verified that Tozasertib treatment decreased the expression of MIF on melanoma cells and CD74 on  $CD4^{+}$  T cell.

In conclusion, this study revealed that AURKB, in addition to promoting the cell cycle, can also inhibit anti-tumor immune responses by increasing the number of tumor-infiltrating  $T_{reg}$  cells by enhancing the MIF-CD74/CXCR4 inhibitory signaling pathway. AURKB inhibitors may be developed as novel anti-tumor immunity drugs and may synergize with immune checkpoint antibodies for melanoma treatment. Moreover, inhibition of MIF was confirmed to be an effective strategy for overcoming resistance to ICB therapy in melanoma [46]. However, further studies are needed to ascertain the specific molecular mechanism of the MIF/CXCR4 pathway following AURKB inhibitor treatment, as well as the synergistic anti-melanoma effect of combining AURKB inhibitors with approved anti-tumor immune-modulating drugs. Our findings provide novel targets and potential drugs for melanoma immunotherapy.

## Funding

This work was supported by National Natural Science Foundation of China (82104453); the Red Medical Famous teacher of Army Medical University (Rong Zhang); the Red Medical Talent Project of Army Medical University (Wuyi Liu) and the Chongqing Key Specialty Construction Project of Clinical Pharmacy (Clinical Pharmacy of Medical oncology).

## CRediT authorship contribution statement

**Qiaoling Wang:** Writing – original draft, Validation, Formal analysis, Data curation, Conceptualization. **Wuyi Liu:** Writing – review & editing, Methodology, Funding acquisition, Data curation, Conceptualization. **Huyue Zhou:** Methodology, Data curation. **Wenjing Lai:** Methodology, Data curation. **Changpeng Hu:** Methodology. **Yue Dai:** Methodology. **Guobing Li:** Writing – review & editing, Conceptualization. **Rong Zhang:** Funding acquisition. **Yu Zhao:** Supervision.

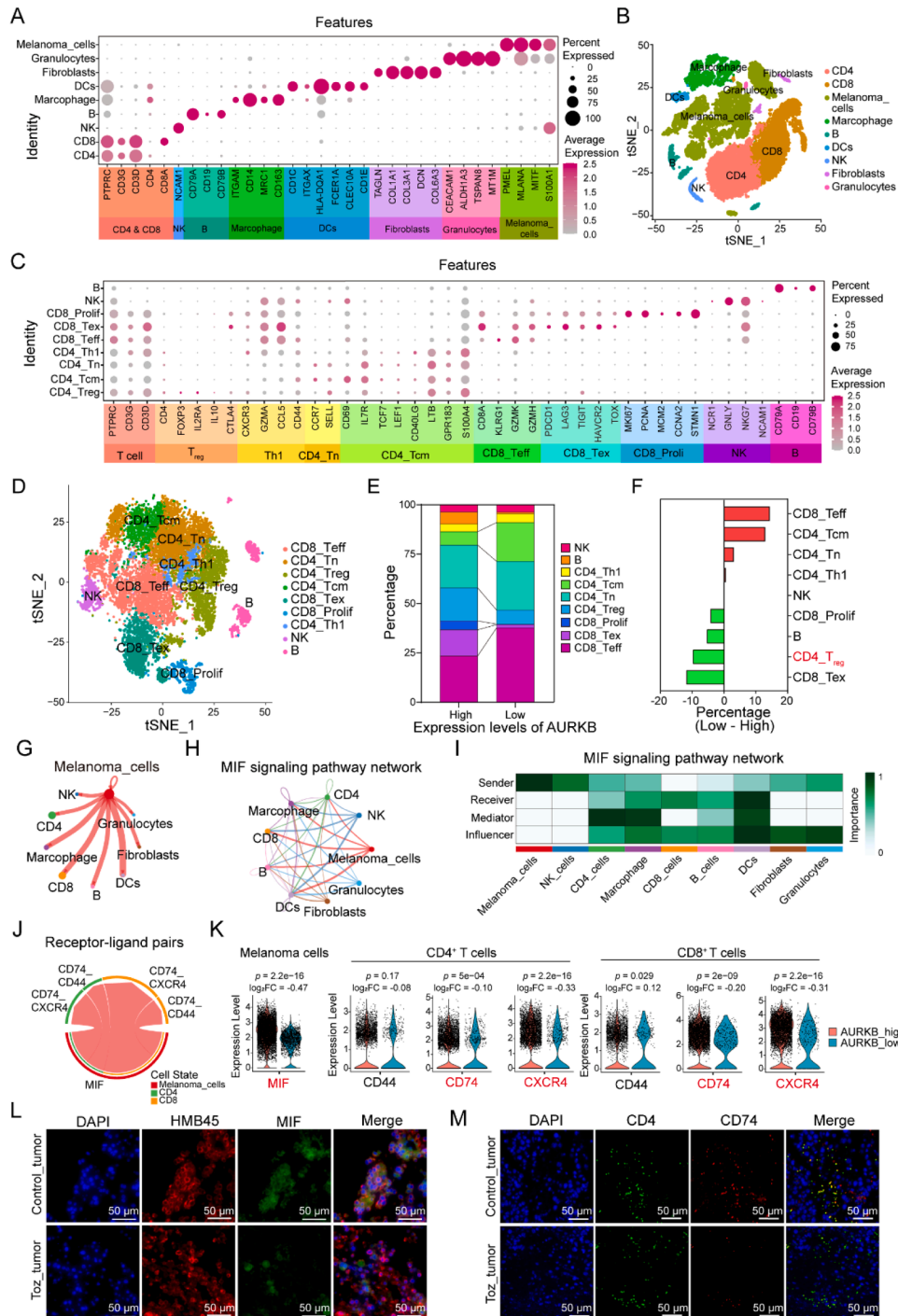


**Fig. 8.** AURKB may increase tumor-infiltrated T<sub>reg</sub> cells through enhancing MIF-CD74/CXCR4 signal communication according to single-cell analysis. (A) Marker genes expression levels of each cell type. (B) The t-SNE reducing dimensionality analysis of all cells in melanoma tissues. (C) The marker gene expression of lymphocyte subpopulation. (D) t-SNE plot of lymphocyte subpopulation clusters. (E, F) The different proportions of subclusters in AURKB high-expression and AURKB low-expression groups. (G) Circle plots present the cell-to-cell communication between cell populations. (H) Circle plots of MIF signaling pathway network. (I) Heatmap shows the relative contribution of MIF signaling network in different cell types. (J) Chord diagram of receptor-ligand pairs in MIF signaling pathway between melanoma cells and CD4<sup>+</sup>, CD8<sup>+</sup> T cells. (K) Violin plots show the different expression of MIF in melanoma cells, CD44, CD74 and CXCR4 in CD4<sup>+</sup> or CD8<sup>+</sup> T cells between AURKB high and low-expression level groups. (L) The different expression levels of MIF on melanoma cells between control and Tozasertib treatment groups. (M) The different expression levels of CD74 on CD4<sup>+</sup> T cells between control and Tozasertib treatment groups.

**Declaration of competing interest**

The authors declare that the research was conducted in the absence of any commercial or financial relationships that could be construed as a potential conflict of interest.

**Supplementary materials**

Supplementary material associated with this article can be found, in the online version, at [doi:10.1016/j.neo.2024.100966](https://doi.org/10.1016/j.neo.2024.100966).

## References

- [1] J. Xu, et al., RAI14 promotes melanoma progression by regulating the FBXO32/c-MYC pathway, *Int. J. Mol. Sci.* 23 (2022).
- [2] W. Guo, H. Wang, C. Li, Signal pathways of melanoma and targeted therapy, *Signal Transduct. Target Ther.* 6 (2021) 424.
- [3] H. Sung, et al., Global cancer statistics 2020: GLOBOCAN estimates of incidence and mortality worldwide for 36 cancers in 185 countries, *CA Cancer J. Clin.* 71 (2021) 209–249.
- [4] M.L. Salgaller, J.S. Weber, S. Koenig, J.R. Yannelli, S.A. Rosenberg, Generation of specific anti-melanoma reactivity by stimulation of human tumor-infiltrating lymphocytes with MAGE-1 synthetic peptide, *Cancer Immunol. Immunother.* 39 (1994) 105–116.
- [5] E. Blass, P.A. Ott, Advances in the development of personalized neoantigen-based therapeutic cancer vaccines, *Nat. Rev. Clin. Oncol.* 18 (2021) 215–229.
- [6] M.K. Callahan, et al., Nivolumab plus ipilimumab in patients with advanced melanoma: updated survival, response, and safety data in a phase I dose-escalation study, *J. Clin. Oncol.* 36 (2018) 391–398.
- [7] J.D. Wolchok, et al., Nivolumab plus ipilimumab in advanced melanoma, *N. Engl. J. Med.* 369 (2013) 122–133.
- [8] R.S. Riley, C.H. June, R. Langer, M.J. Mitchell, Delivery technologies for cancer immunotherapy, *Nat. Rev. Drug Discov.* 18 (2019) 175–196.
- [9] F. Martins, et al., Adverse effects of immune-checkpoint inhibitors: epidemiology, management and surveillance, *Nat. Rev. Clin. Oncol.* 16 (2019) 563–580.
- [10] R.D. Carvajal, A. Tse, G.K. Schwartz, Aurora kinases: new targets for cancer therapy, *Clin. Cancer Res.* 12 (2006) 6869–6875.
- [11] C.H. Kim, et al., Mitotic protein kinase-driven crosstalk of machineries for mitosis and metastasis, *Exp. Mol. Med.* 54 (2022) 414–425.
- [12] E.A. Harrington, et al., VX-680, a potent and selective small-molecule inhibitor of the Aurora kinases, suppresses tumor growth *in vivo*, *Nat. Med.* 10 (2004) 262–267.
- [13] L. Ding, H. Gu, X. Gao, S. Xiong, B. Zheng, Aurora kinase a regulates m1 macrophage polarization and plays a role in experimental autoimmune encephalomyelitis, *Inflammation* 38 (2015) 800–811.
- [14] T.T. Glant, et al., Differentially expressed epigenome modifiers, including aurora kinases A and B, in immune cells in rheumatoid arthritis in humans and mouse models, *Arthritis Rheum.* 65 (2013) 1725–1735.
- [15] A.N. Polat, et al., Phosphoproteomic analysis of aurora kinase inhibition in monopolar cytokinesis, *J. Proteome Res.* 14 (2015) 4087–4098.
- [16] N. Pishesha, T.J. Harmand, H.L. Ploegh, A guide to antigen processing and presentation, *Nat. Rev. Immunol.* 22 (2022) 751–764.
- [17] A. Sharabi, et al., Regulatory T cells in the treatment of disease, *Nat. Rev. Drug Discov.* 17 (2018) 823–844.
- [18] G.P. Dunn, L.J. Old, R.D. Schreiber, The immunobiology of cancer immunosurveillance and immunoediting, *Immunity* 21 (2004) 137–148.
- [19] M. Giulietti, et al., Emerging biomarkers in bladder cancer identified by network analysis of transcriptomic data, *Front. Oncol.* 8 (2018) 450.
- [20] K. Du, et al., Pathway signatures derived from on-treatment tumor specimens predict response to anti-PD1 blockade in metastatic melanoma, *Nat. Commun.* 12 (2021) 6023.
- [21] L. Lin, et al., Ferroptosis-related NFE2L2 and NOX4 genes are potential risk prognostic biomarkers and correlated with immunogenic features in glioma, *Cell Biochem. Biophys.* 81 (2023) 7–17.
- [22] M. Oshi, et al., G2M checkpoint pathway alone is associated with drug response and survival among cell proliferation-related pathways in pancreatic cancer, *Am. J. Cancer Res.* 11 (2021) 3070–3084.
- [23] H. Yi, Y. Zhen, L. Jiang, J. Zheng, Y. Zhao, The phenotypic characterization of naturally occurring regulatory CD4+CD25+ T cells, *Cell. Mol. Immunol.* 3 (2006) 189–195.
- [24] A. Sarvaria, J.A. Madrigal, A. Saudemont, B cell regulation in cancer and anti-tumor immunity, *Cell. Mol. Immunol.* 14 (2017) 662–674.
- [25] S. Downs-Canner, et al., Suppressive IL-17A(+)Foxp3(+) and ex-Th17 IL-17A(neg) Foxp3(-) T(reg) cells are a source of tumour-associated T(reg) cells, *Nat. Commun.* 8 (2017) 14649.
- [26] I. Smalley, et al., Single-cell characterization of the immune microenvironment of melanoma brain and leptomeningeal metastases, *Clin. Cancer Res.* 27 (2021) 4109–4125.
- [27] C. Liongue, T. Taznin, A.C. Ward, Signaling via the CytoR/JAK/STAT/SOCS pathway: emergence during evolution, *Mol. Immunol.* 71 (2016) 166–175.
- [28] S. Jin, et al., Inference and analysis of cell-cell communication using CellChat, *Nat. Commun.* 12 (2021) 1088.
- [29] J. Couzin-Frankel, Breakthrough of the year 2013. Cancer immunotherapy, *Science* 342 (2013) 1432–1433.
- [30] B.F. Zamarron, W. Chen, Dual roles of immune cells and their factors in cancer development and progression, *Int. J. Biol. Sci.* 7 (2011) 651–658.
- [31] B. Goldenson, J.D. Crispino, The aurora kinases in cell cycle and leukemia, *Oncogene* 34 (2015) 537–545.
- [32] K. Tsuboi, et al., A phase I study to assess the safety, pharmacokinetics and efficacy of barasertib (AZD1152), an Aurora B kinase inhibitor, in Japanese patients with advanced acute myeloid leukemia, *Leuk. Res.* 35 (2011) 1384–1389.
- [33] F.J. Giles, et al., MK-0457, an Aurora kinase and BCR-ABL inhibitor, is active in patients with BCR-ABL T315I leukemia, *Leukemia* 27 (2013) 113–117.
- [34] H.J. Meulenbeld, et al., Randomized phase II study of danusertib in patients with metastatic castration-resistant prostate cancer after docetaxel failure, *BJU Int.* 111 (2013) 44–52.
- [35] U.A. Matulonis, et al., ENMD-2076, an oral inhibitor of angiogenic and proliferation kinases, has activity in recurrent, platinum resistant ovarian cancer, *Eur. J. Cancer* 49 (2013) 121–131.
- [36] S. Punt, et al., Aurora kinase inhibition sensitizes melanoma cells to T-cell-mediated cytotoxicity, *Cancer Immunol. Immunother.* 70 (2021) 1101–1113.
- [37] R. Du, C. Huang, K. Liu, X. Li, Z. Dong, Targeting AURKA in cancer: molecular mechanisms and opportunities for cancer therapy, *Mol. Cancer* 20 (2021) 15.
- [38] J. Han, et al., Inhibition of aurora-A promotes CD8(+) T-cell infiltration by mediating IL10 production in cancer cells, *Mol. Cancer Res.* 18 (2020) 1589–1602.
- [39] T. Yin, et al., Aurora A inhibition eliminates myeloid cell-mediated immunosuppression and enhances the efficacy of anti-PD-L1 therapy in breast cancer, *Cancer Res.* 79 (2019) 3431–3444.
- [40] C. Li, P. Jiang, S. Wei, X. Xu, J. Wang, Regulatory T cells in tumor microenvironment: new mechanisms, potential therapeutic strategies and future prospects, *Mol. Cancer* 19 (2020) 116.
- [41] C.C. Nobre, et al., Macrophage migration inhibitory factor (MIF): biological activities and relation with cancer, *Pathol. Oncol. Res.* 23 (2017) 235–244.
- [42] J.D. Marshall, et al., Complexity of macrophage migration inhibitory factor (MIF) and other angiogenic biomarkers profiling in pulmonary arterial hypertension, *Pulm. Circ.* 7 (2017) 730–733.
- [43] K. Yaddanapudi, et al., MIF is necessary for late-stage melanoma patient MDSC immune suppression and differentiation, *Cancer Immunol. Res.* 4 (2016) 101–112.
- [44] H. Huai, J. Li, J. Li, H. Lan, Transcriptome analysis and single-cell sequencing analysis constructed the metastasis-related signature in melanoma and identified CD74 as a novel biomarker (2023).
- [45] C.R. Figueiredo, et al., Blockade of MIF-CD74 signalling on macrophages and dendritic cells restores the antitumor immune response against metastatic melanoma, *Front. Immunol.* 9 (2018) 1132.
- [46] R.A. de Azevedo, et al., MIF inhibition as a strategy for overcoming resistance to immune checkpoint blockade therapy in melanoma, *Oncoimmunology* 9 (2020) 1846915.